Microfluidic droplet sorting using integrated bilayer micro-valves

Yuncong Chen, Yang Tian, Zhen Xu, Xinran Wang, Sicong Yu, and Liang Dong

Citation: Appl. Phys. Lett. **109**, 143510 (2016); doi: 10.1063/1.4964644
View online: http://dx.doi.org/10.1063/1.4964644
View Table of Contents: http://aip.scitation.org/toc/apl/109/14
Published by the American Institute of Physics

RIGHTSLINK

Microfluidic droplet sorting using integrated bilayer micro-valves

Yuncong Chen,[a] Yang Tian,[a] Zhen Xu, Xinran Wang, Sicong Yu, and Liang Dong[b]
Department of Electrical and Computer Engineering, Iowa State University, Ames, Iowa 50011, USA

(Received 24 June 2016; accepted 28 September 2016; published online 7 October 2016)

This paper reports on a microfluidic device capable of sorting microfluidic droplets utilizing conventional bilayer pneumatic micro-valves as sorting controllers. The device consists of two micro-valves placed symmetrically on two sides of a sorting area, each on top of a branching channel at an inclined angle with respect to the main channel. Changes in transmitted light intensity, induced by varying light absorbance by each droplet, are used to divert the droplet from the sorting area into one of the three outlet channels. When no valve is activated, the droplet flows into the outlet channel in the direction of the main channel. When one of the valves is triggered, the flexible membrane of valve will first be deflected. Once the droplet leaves the detection point, the deflected membrane will immediately return to its default flattened position, thereby exerting a drawing pressure on the droplet and deviating it from its original streamline to the outlet on the same side as the valve. This sorting method will be particularly suitable for numerous large-scale integrated microfluidic systems, where pneumatic micro-valves are already used. Only few structural modifications are needed to achieve droplet sorting capabilities in these systems. Due to the mechanical nature of diverting energy applied to droplets, the proposed sorting method may induce only minimal interference to biological species or microorganisms encapsulated inside the droplets that may accompany electrical, optical and magnetic-based techniques. *Published by AIP Publishing.*
[http://dx.doi.org/10.1063/1.4964644]

Sorting micro/nano-particles and micro-droplets from a large population with high efficiency and accuracy is highly desirable for microfluidic devices that have applications such as high-throughput biological assays, chemical reactions and processing, and environmental assessments. Existing sorting mechanisms can be classified as passive, active, and combined means.[1] Passive sorting does not require external fields but instead utilizes interactive effects between particles/droplets, flow field and channel structures or relies on differences in the density and size of different particles. For instance, the pinched flow fractionation method employs the characteristics of laminar flow and difference in particle size to separate particles in a channel.[2] Deterministic lateral displacement is a steric method of continuous separation that makes use of asymmetric bifurcation of laminar flow around the obstacles.[3] In contrast, active sorting requires external fields in various forms and offers higher sorting accuracy. Remarkable active means of sorting include using dielectrophoresis, under electric fields,[4,5] and applying magnetic fields to differentiate particles, based on their magnetic properties.[6,7] Optical, acoustic, and mechanical methods have also been used to achieve sorting.[8–13] To improve sorting efficiency, some passive means of sorting also utilize external fields.[14–16] A modification to the pinched flow fractionation method involves applying a laser beam to particles for improved sorting efficiency.[15,16]

Notably, the pneumatic micro-valve developed by Quake *et al.*[17] has become a widely used on-chip valving method in many biochip applications. This valve involves a bilayer polydimethylsiloxane (PDMS) structure, where liquid flows inside the bottom layer while the upper layer integrates an air network. Between the bottom and upper layers is a thin flexible membrane. To activate the valve, compressed air is pumped into the air channel such that the membrane is forced to bend towards the liquid flow channel. This operation allows compressing and clogging of channels in the fluidic layer to manipulate liquid flow. Such valves have been extensively utilized as active components to perform valving, chopping, switching, and pumping[18,19] in the integrated microfluidic systems.[17]

In this paper, we report a means of sorting microdroplets utilizing bilayer pneumatic micro-valves. The proposed droplet sorter shown in Fig. 1(a) consists of a main inlet channel and three outlet channels. Two valves, i.e., V1 and V2, are placed on two side-channels at an inclined angle with respect to the main channel, serving as sorting controllers. These channels meet at a droplet sorting area. The two control valves are set to be normally opened with flat membranes. An optical detection setup is used to determine the direction of diverting a target droplet away from the sorting area into one of the three outlet channels, where a laser beam originating from the top of the device is aimed as a detection spot (indicated by green circle in Fig. 1(a)) located at the end of the main channel near the sorting area (indicated by a dashed red circle). When a droplet in Fig. 1(b) arrives at the detection point from the main channel, it attenuates transmitted light signals based on its light absorbance and/or scattering characteristics. The transmitted light intensity (TLI) is detected by a photodetector (model 1918; Newport Power Meter) on the lower side of the sorter. If the change in the TLI is more than a pre-determined trigger value, then a valve will be triggered to turn on and pneumatically deflect the membrane (Fig. 1(c)). In this moment, the droplet movement

[a]Y. Chen and Y. Tian contributed equally to this work.
[b]Author to whom correspondence should be addressed. Electronic mail: ldong@iastate.edu.

RIGHTSLINK

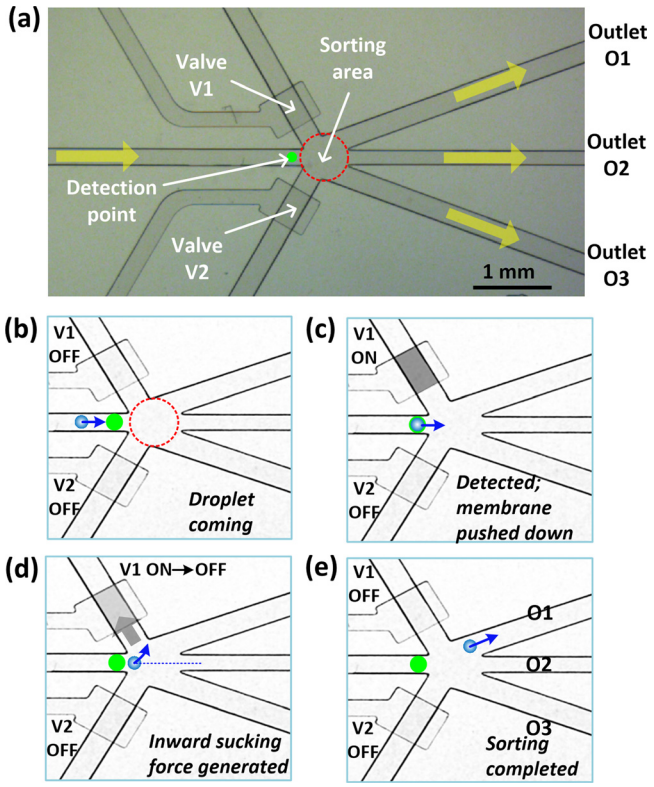

FIG. 1. (a) Photograph of the proposed micro-droplet sorter. The green dot and the dashed red circle represent the optical detection point and the sorting area, respectively. (b)–(d) Schematic of the sorting processes. The blue dot represents a target water droplet carried by an oil phase flow. The gray arrow in (d) at the valve represents the inward drawing pressure generated during the relaxation of the deflected membrane.

is not deviated from the streamline yet because it still remains in the main channel. However, once the droplet leaves the detection point and immediately enters the sorting area, the change in the TLI will become less than the pre-set value. As a result, the valve will be deflated and the membrane will return upward to its default flattened position, thereby exerting a drawing force on the droplet (Fig. 1(d)). The droplet will thus deviate from its original streamline to flow into the collection channel on the same side as the activated valve (Fig. 1(e)). Therefore, by pre-setting two different trigger values for the two valves, droplets with different light absorbance and scattering characteristics can be diverted to either outlet O1 or O3. Without any operations of the valves, the droplets-containing flow coming from the main channel will enter into outlet O2 oriented along the main channel. This sorting mechanism was also illustrated using a finite element method based simulation, as described in the supplementary material.

Fig. 2(a) shows the setup of the sorting system. Electrically activated solenoids (S10 MM-31–12-3/A; Pneumadyne, Plymouth, MN) were used to control the valves. The solenoids were connected to a compressed air source and fed by the electrical signal output of the photodetector. To generate droplets with different optical properties, the microfluidic device contained an alternating droplet generator (ADG)[20] with two cross-junction droplet generation units at the upstream end of the main channel (Fig. 2(b)). Fig. 2(c) shows the electronic circuit that amplifies the signals from the photodetector and then compares them with the pre-set trigger voltages. In our experiments, three different water solutions were prepared by mixing black food-dye solution (AmeriColor) with deionized (DI) at different volume ratios of 10%, 5%, and 0.5%. Single color droplets were produced by one generation unit on the ADG, while generating droplets with two different colors required use of both generation units. The fabrication processes for the PDMS sorter is described in the supplementary material.

We first assessed the ability of the sorter to direct a train of droplets with the same color into a designated outlet. The

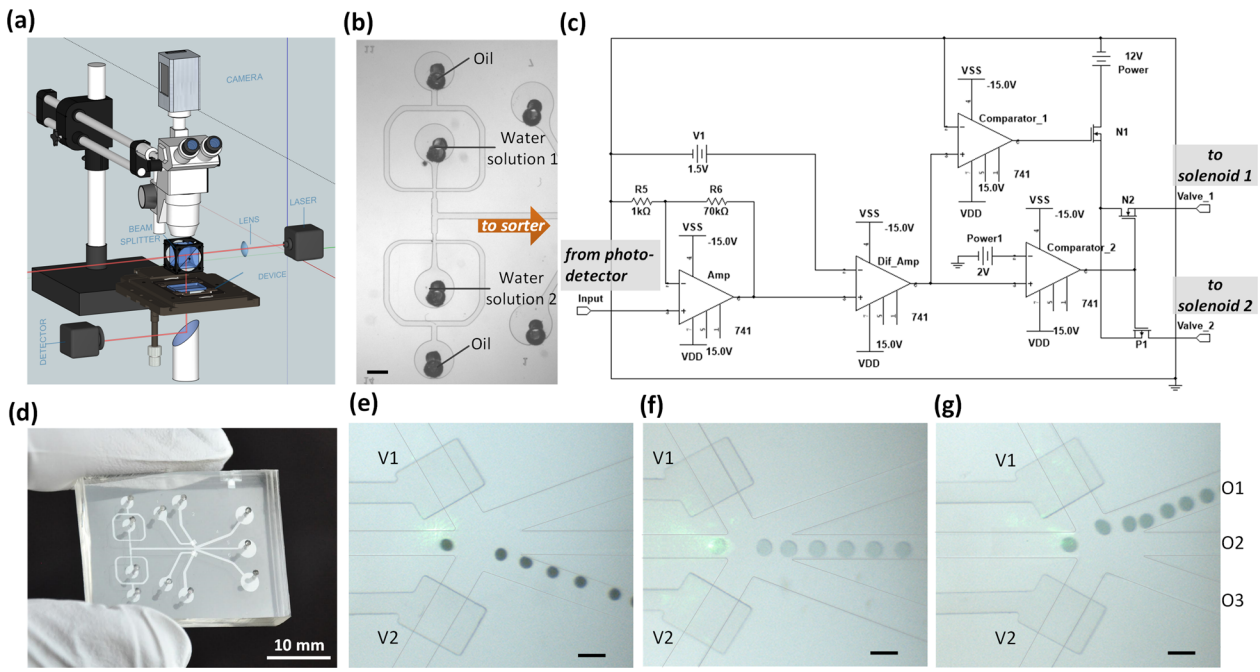

FIG. 2. (a) Schematic of the setup for the proposed droplet sorter. (b) Photograph of an ADG used to produce different color droplets to test the sorter. The scale bar represents 700 μm. (c) Electronic circuit used to control the states of the valves. (d) Photograph of the sorter. (e)–(g) Directing a train of droplets with the same color into different outlet channels based on the gray level of the droplets: dark (e), light (f), and mediate (g) levels. The scale bars represent 300 μm.

RIGHTSLINK

pre-set trigger voltages at the output of the amplifier circuit for driving valves V1 and V2 were 1.8 V and 1.2 V, respectively. When no droplets flowed through the detection area, the output voltage was 2.4 V. In Fig. 2(e), when the dark droplets passed through the detection point, the output voltage value decreased to lower than 1.2 V, constituting a 54% reduction in the TLI, and thus, V2 was triggered to divert the droplets into outlet O3, while V1 remained in the "off" state. As another train of light droplets in Fig. 2(f) flowed through the detection point, the resulting 12% reduction in the TLI was not significant enough to bring the output voltage below 1.8 V, and thus no valves were triggered. As a result, the light droplets flowed downstream into outlet O2 (Fig. 2(f)). When the mediate color droplets arrived at the sorting area, a 31% reduction in the TLI occurred that caused the voltage to decrease to 1.5 V, thus triggering V2 but not V1. As expected, the mediate color droplets were directed to outlet O1 (Fig. 2(g)).

Next, we investigated whether or not the sorter could extract the desired droplets from a stream of droplets with mixed colors. Fig. 3(a) shows that the droplets of two gray levels were produced by the ADG and alternatively flowed into the main channel. Fig. 3(b) shows that the mediate color droplets were directed by valve V2 into outlet O1, while the light color droplets continued flowing into outlet O2 in the middle. Fig. 3(c) shows that the dark droplets were redirected by V1 and flowed into outlet O3, while the light ones flowed into the middle outlet channel O2. The images in Fig. 3 were extracted from the movies available in supplementary material. In this experiment, the pre-set voltages for triggering V1 and V2 were the same as those of the previous experiment at 1.8 V and 1.2 V, respectively. To visualize each critical step of the entire sorting process, detailed decompositions are provided in Fig. 3(d). A mediate color droplet (indicate by a red arrow) arrived at the detection point at

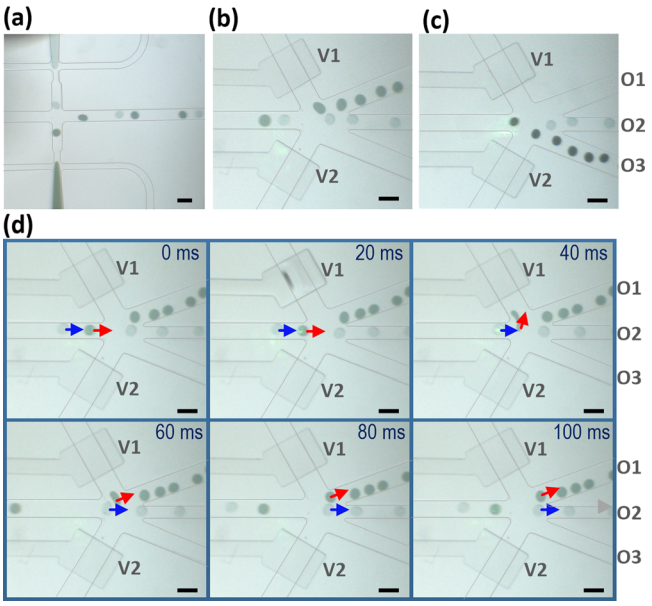

FIG. 3. (a) Photograph of generating droplets with alternating colors. (b) Sorting mediate and light color droplets to outlet O1 and O2, respectively. (c) Sorting light and dark color droplets to outlet O2 and O3, respectively. (d) Time-lapse images for sorting a mediate color droplet (indicated by a red arrow) to outlet O1 and the following light droplet (blue arrow) to outlet O2. The scale bars represent 300 μm.

20 ms, triggering the initially flat membrane of V1 to deflect downward. Once the droplet left the detection point, the membrane returned flat to draw the droplet towards the valve at 40 ms, during which the droplet was deformed by the drawing pressure. Almost at the same time, a light color droplet (indicated by a blue arrow) arrived at the detection point. But, none of the valves were triggered owing to the inadequate change in the TLI at 60 ms. Thus, this droplet did not deviate from its original flow direction and entered outlet O2 at 80 ms. At this time, the initial droplet had already flowed inside the channel of outlet O1.

In the experiments described above, the detection point was located at the end of the main channel and the inward sucking pressure was created from the relaxation of the deflected valve membrane and exerted upon a target droplet for sorting. In another trial shown in Fig. 4, the detection point was relocated into the sorting area and the outward pushing pressure generated during the downward deflection of the membrane was instead used to divert a target droplet. The results show that when a mediate color droplet entered the sorting area, valve V2 was triggered to deflect its membrane pushing away the droplet (Figs. 4(a), 4(b), 4(e), and 4(f)). But, after the droplet left the detection point, the membrane of V2 immediately returned upward to the flat position, during which the accompanying sucking pressure by V2 was applied to the droplet, thus drawing it backwards (Figs. 4(c) and 4(g)). Therefore, the droplet in Figs. 4(d) and 4(h) was incorrectly directed into outlet O2. Similarly, an inward sucking pressure generated during the relaxation of the deflected membrane also failed to draw a target droplet into the outlet on the same side of the valve. Therefore, this mode of operation in Fig. 4 would not be recommended to use in sorting.

Fig. 5 shows that the proposed droplet sorter was capable of achieving an almost 100% success rate when sorting frequency was no more than $f = 20$ Hz. Here, sorting frequency is defined as the number of droplets passing through the detection point within 1 s. As the sorting frequency further increased, the success rate of sorting decreased. At $f = 25$ Hz, the sorting error rate was ~12%. Although the detection electronics of the system provided a microsecond-scale response time, the pneumatic valve was not fast enough to correctly respond to an operation instruction by switching between its "on" and "off" states at a higher sorting frequency. In addition, sorting accuracy of the system depends on detection accuracy of the photodetector used. The photodetector provides an accuracy of ±0.2% for continuous wave mode, which could be translated into a voltage variation of ±0.14 V at the output of our amplifier circuit shown in Fig. 2(c). Given the diameter (~250 μm) of the laser beam, if the target droplet is too small to introduce sufficient changes in TLI (and thus voltage variation), the system would not be able to correctly perform the sorting of droplets. Therefore, increasing accuracy of the photodetector and/or decreasing the detection beam size would allow the system to sort smaller droplets. Furthermore, in our system, each droplet was 0.15 mm in diameter, the linear flow rate of carrier oil was ~8 mm/s, and the obtained highest sorting frequency was 20 Hz. Assume that the droplets in the main channel were periodically spaced. The minimum space between neighboring droplets for sorting

RIGHTSLINK

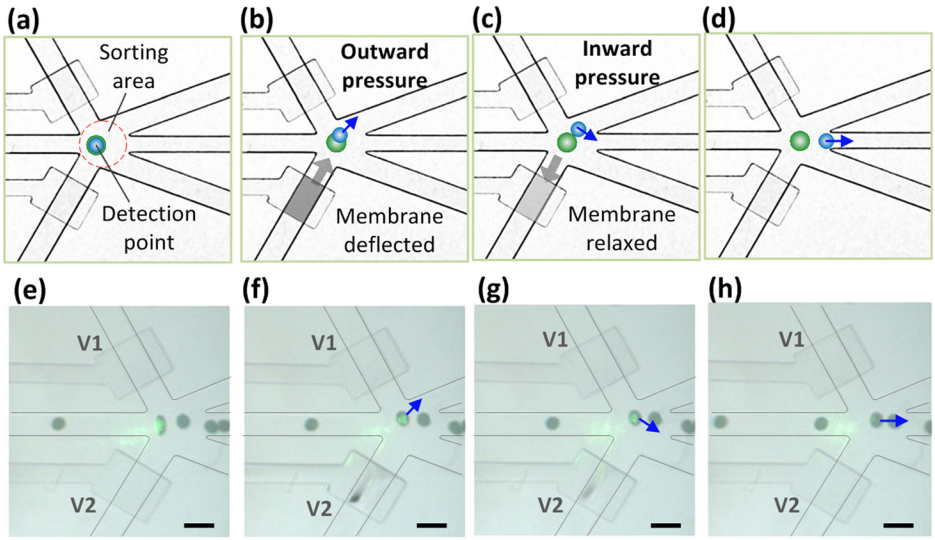

FIG. 4. (a)–(d) Decompositions of droplet sorting based on using the outward pressure to drive a target droplet into a desired outlet channel. The detection point was located in the sorting area. (e)–(d) Time-lapse images of droplet sorting correspondingly described in (a)–(d). In (f), the outward pressure was generated as the membrane of V2 was deflected downward. In (c), before the droplet completely left the detection area, the inward pressure generated during the relaxation of the membrane pulled the droplet back to the sorting area. The scale bars represent 300 μm.

would thus be (8 mm/20) − 0.15 mm = 0.25 mm. Droplet sorting at a lower frequency would require a shorter minimum distance between the neighboring droplets. Also, when any one of the control valves was turned on, the pressure in the sorting area increased and the total pressure drop across the main channel decreased. This, in turn, would reduce the flow velocity of droplets. Therefore, temporary reduction of the distance between the neighboring droplets might occur during inflating of the triggered valve. But, once the target droplet passed through the optical detection point, the valve would immediately recover to its flat state. This would relax the temporarily increased pressure in the main channel, and thus the distance between the neighboring droplets would increase back to the original value. Therefore, continuous sorting of droplets could be obtained.

Compared to the previously reported two mechanical sorters using vertical wall based in-plane pneumatic valves,[12,13] our bilayer valve based sorter provided a higher sorting frequency than the one with five sampling outlets (~2 Hz),[12] but lower than the other with two sampling outlets (~250 Hz).[13] The moderate sorting frequency of our sorter may perhaps be caused by the indirect body contact of the droplets with the valves and the moderate number of sampling outlets. It should be noted that although the in-plane pneumatic valves have a simpler structure,[21] each valve often requires an individual control, which may cause complexity in designing large-scale microfluidic systems[22] with multiple sorters and other units. In contrast, the bilayer valves adopted in our sorter need relatively complex fabrication processes, but they are known for addressable control to reduce layout complexity of pneumatic lines used in microfluidic large-scale integration.[17,22] Therefore, the proposed sorter will be particularly suitable for integration into complex microfluidic systems that use pneumatic bilayer valves.[17,22] With only a few structural modifications, droplet sorting capabilities, when needed, will be readily achieved in these systems.

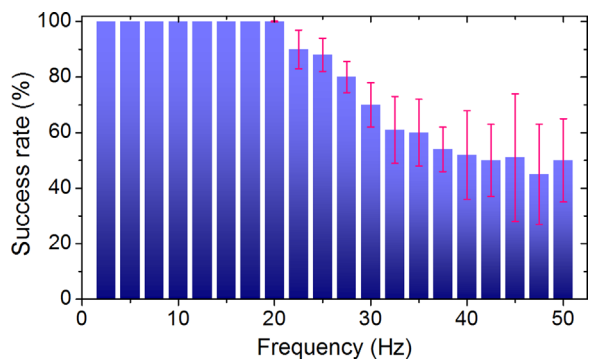

FIG. 5. Sorting error analysis based sorting success rate as a function of sorting frequency. Error bars represent standard deviation obtained from sorting 10^3 droplets.

The potential applications of the proposed microfluidic droplet sorter are widespread since the mechanical means of droplet sorting may induce minimal interference to biological species or microorganisms[23,24] encapsulated inside droplets that often accompany many other active separation and sorting devices using electrical, optical and magnetic driving forces. Future work includes applying this microfluidic sorter to sort the droplets containing cells whose growth density may influence the TLI and thus trigger sorting. It is also our interest to integrate this sorting method with other sensing mechanisms, such as fluorescence detection, to develop a flow cytometer-like device for sorting droplets.

See supplementary material for three movies showing the sorting processes, the fabrication processes for the microfluidic sorter, and the hydrodynamic simulation results.

This work was supported in part by the Plant Sciences Institute and the Institute for Physical Research and Technology at Iowa State University and the National Science Foundation under Grant Nos. ECCS-1102354, ISO-1650182, and DBI-1353819. The authors also thank Dr. Zhiyou Wen, Dr. Laura Jarboe, and Dr. Daniel Attinger for their helpful discussions.

[1]P. Sajeesh and A. K. Sen, Microfluid. Nanofluid. **17**, 1–52 (2014).
[2]J. Oakey, J. Allely, and D. W. Marr, Biotechnol. Prog. **18**, 1439–1442 (2002).
[3]L. R. Huang, E. C. Cox, R. H. Austin, and J. C. Sturm, Science **304**, 987–990 (2004).
[4]X. B. Wang, Y. Huang, F. F. Becker, and P. R. C. Gascoyne, J. Phys. D: Appl. Phys. **27**, 1571 (1994).

RIGHTSLINK

[5]X. B. Wang, J. Yang, Y. Huang, J. Vykoukal, F. F. Becker, and P. R. C. Gascoyne, Anal. Chem. **72**, 832–839 (2000).
[6]K. Smistrup, T. Lund-Olesen, M. F. Hansen, and P. T. Tang, J. Appl. Phys. **99**, 08P102 (2006).
[7]M. Bu, T. B. Christensen, K. Smistrup, A. Wolff, and M. F. Hansen, Sens. Actuators, A **145**, 430–436 (2008).
[8]O. Brzobohatý, V. Karásek, M. Šiler, L. Chvátal, T. Čižmár, and P. Zemánek, Nat. Photonics **7**, 123–127 (2013).
[9]A. Lenshof, C. Magnusson, and T. Laurell, Lab Chip **12**, 1210–1223 (2012).
[10]S. Li, X. Ding, F. Guo, Y. Chen, M. I. Lapsley, S. C. S. Lin, W. Lin, J. P. McCoy, C. E. Cameron, and T. J. Huang, Anal. Chem. **85**, 5468–5474 (2013).
[11]Q. Zhang, P. R. Zhang, Y. T. Su, M. L. Yang, and B. Ma, Lab Chip **14**, 4599–4603 (2014).
[12]D. H. Yoon, D. Wakui, A. Nakahara, T. Sekiguchi, and S. Shoji, RSC Adv. **5**, 2070–2074 (2015).
[13]A. R. Abate, J. J. Agresti, and D. A. Weitz, Appl. Phys. Lett. **96**, 203509 (2010).
[14]Z. Wu, A. Q. Liu, and K. Hjort, J. Micromech. Microeng. **17**, 1992 (2007).
[15]A. Y. Lau, L. P. Lee, and J. W. Chan, Lab Chip **8**, 1116–1120 (2008).
[16]K. H. Lee, S. B. Kim, K. S. Lee, and H. J. Sung, Lab Chip **11**, 354–357 (2011).
[17]M. A. Unger, H. P. Chou, T. Thorsen, A. Scherer, and S. R. Quake, Science **288**, 113–116 (2000).
[18]C. W. Lai, Y. H. Lin, and G. B. Lee, Biomed. Microdevices **10**, 749–756 (2008).
[19]O. C. Jeong and S. Konishi, Sens. Actuators, A **135**, 849–856 (2007).
[20]D. R. Link, E. Grasland-Mongrain, A. Duri, F. Sarrazin, Z. Cheng, G. Cristobal, M. Marquez, and D. A. Weitz, Angew. Chem., Int. Ed. **45**, 2556–2560 (2006).
[21]A. R. Abate, M. B. Romanowsky, J. J. Agresti, and D. A. Weitz, Appl. Phys. Lett. **94**, 023503 (2009).
[22]T. Thorsen, S. J. Maerkl, and S. R. Quake, Science **298**, 580–584 (2002).
[23]H. Yang, X. Qiao, M. K. Bhattacharyya, and L. Dong, Biomicrofluidics **5**, 044103 (2011).
[24]P. Liu, R. J. Martin, and L. Dong, Lab Chip **13**, 650–661 (2013).

RIGHTSLINK